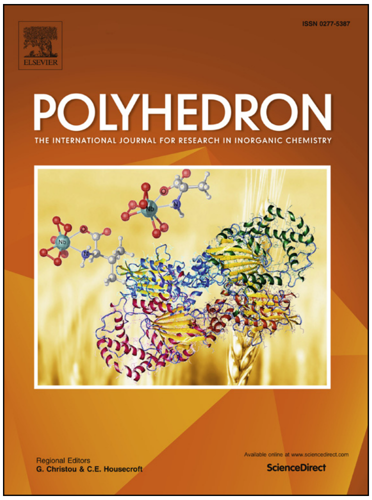

Synthesis, Characterization and Reactivity of Halides/Pseudohalides and their Complexes Containing Ruthenium II in the Hydrogenation of Cyclohexene

Murillo C. Ribeiro, Rodrigo S. Corrêa, Marília I.F. Barbosa, Javier Ellena, André L. Bogado, Alzir A. Batista

PII: S0277-5387(17)30544-2
DOI: http://dx.doi.org/10.1016/j.poly.2017.08.013
Reference: POLY 12777

To appear in: *Polyhedron*

Received Date: 10 June 2017
Revised Date: 1 August 2017
Accepted Date: 17 August 2017

Please cite this article as: M.C. Ribeiro, R.S. Corrêa, M.I.F. Barbosa, J. Ellena, A.L. Bogado, A.A. Batista, Synthesis, Characterization and Reactivity of Halides/Pseudohalides and their Complexes Containing Ruthenium II in the Hydrogenation of Cyclohexene, *Polyhedron* (2017), doi: http://dx.doi.org/10.1016/j.poly.2017.08.013

Synthesis, Characterization and Reactivity of Halides/Pseudohalides and their Complexes Containing Ruthenium II in the Hydrogenation of Cyclohexene

Murillo C. Ribeiro[a], Rodrigo S. Corrêa[b], Marília I. F. Barbosa[♯a], Javier Ellena[c], André L. Bogado[d] and Alzir A. Batista[a]

[a] *Departamento de Química, Universidade Federal de São Carlos, Cx. Postal 676, CEP 13565-905, São Carlos – SP, Brazil*

[b] *Departamento de Química, ICEB, Universidade Federal de Ouro Preto, CEP 35400-000, Ouro Preto - MG, Brazil*

[c] *Instituto de Física de São Carlos-USP, Cx. Postal 780, CEP 13560-970, São Carlos – SP, Brazil*

[d] *Faculdade de Ciências Integradas do Pontal, Universidade Federal de Uberlândia, Rua vinte, 1600, CEP 38304-402 Ituiutaba, MG, Brazil*

Corresponding author: daab@ufscar.br (A.A. Batista), or bogado@ufu.br (A.L. Bogado)

Present address:

♯ Instituto de Química, Universidade Federal de Alfenas, CEP 37130000, Alfenas - MG. Brazil

Abstract

In this paper, the influence of pseudohalide ligands coordinated to the ruthenium center on the hydrogenation of cyclohexene was investigated. The pseudohalide complexes containing ruthenium were synthesized from the *cis*-[RuCl$_2$(dppb)(N-N))] {where N-N = 2,2′-bipyridine (bipy) **(1A)**, 4,4′-dimethyl-2,2′-bipyridine (Me-bipy) **(2)**, or 4,4′-dimethoxy-2,2′-bipyridine (MeO-bipy) **(3)**, dppb = 1,4-bis(diphenylphosphino)butane,} by chloride exchange to provide complexes with general formula *cis*-[RuL$_2$(dppb)(N-N)] {where L$_2$ = N$_3^-$ **(4)**, **(7)** and **(9)** CN$^-$ **(5)**, **(8)** and **(10)** or SCN$^-$ **(6)** and **(11)**}. All complexes were characterized using spectroscopic, electrochemical techniques, as well as elemental analyses to check their molecular formulation and purity. Furthermore, crystal structure of the complexes *cis*-[Ru(N$_3$)$_2$(dppb)(bipy)] (**4**), *cis*-[Ru(CN)$_2$(dppb)(bipy)] (**5**), *cis*-[Ru(SCN)$_2$(dppb)(bipy)] (**6**), *cis*-[Ru(CN)$_2$(dppb)(Me-bipy)] (**8**), and *cis*-[Ru(SCN)$_2$(dppb)(MeO-bipy)] (**11**) were determined by single-crystal X-ray diffraction, as well as the X-ray structure of the solvate complex [RuCl(CH$_3$CN)(dppb)(bipy)](PF$_6$) (**1B**). Dichloride and pseudohalide complexes containing ruthenium were applied as pre-catalysts in the hydrogenation of cyclohexene, after pre-established conditions using the *cis*-[RuCl$_2$(dppb)(bipy)] **(1A)** as a target complex. The quantitative conversion of cyclohexene to cyclohexane was obtained in 5h at 25 °C using 0.1 mol % of **(1A)** in methanol solution at 15 atm H$_2$. The substituted bipy derivatives **(2)** and **(3)** were also effective pre-catalysts, but pseudohalides were not under these conditions.

Keywords: Ruthenium complexes, pseudohalide, solvate complexes, hydrogenation of cyclohexene, molecular structure.

1. Introduction

The hydrogenation of simple or prochiral alkenes is a vital area of research, and ruthenium catalysts have figured prominently in this area. The Wilkinson's catalyst [$RhCl(PPh_3)_3$] is the best-known complex that activates the H_2 molecule by oxidative addition [1,2]. The [$RuCl(dppb)_2(\mu\text{-}Cl)]_2$ complex catalyzes the hydrogenation of styrene [3], the transfer hydrogenation of acetophenone (from propan-2-ol) [4] and H_2-hydrogenation of imines [5]. The first reported "Ru(P-P)" enantioselective catalyst in the hydrogenation of prochiral olefins was the [$\{RuCl(P\text{-}P)\}_2\text{-}\mu\text{-}(Cl)_2$] (P-P = chiraphos, diop and binap) species [5]. Afterwards, many "Ru(P-P)" moieties containing complexes {where P-P = chiral or non-chiral bisphosphine}, such as [$Ru_2Cl_4(P\text{-}P)_2(NEt_3)$] [6], [$Ru(OAc)_2(binap)$] [6,7], [$RuCl(arene)(P\text{-}P)]^+$ [7], [$RuH(P\text{-}P)(solvent)_3]^+$ [8–10], [$Ru(P\text{-}P)(\pi\text{-}allyl)_2$] [11–13], [$RuCl_2(RCN)_2(P\text{-}P)$] [5,14], [$RuX(P\text{-}P)]_2\text{-}\mu\text{-}(X)_2$] (X = halogen) [5,6] and [$RuX(P\text{-}P)]_2(\mu\text{-}X)_3$] [6,15] were used as catalysts in the hydrogenation of functionalized olefins, dienes, and ketones [2,16] and certain prochiral imines [17].

We reported that ruthenium (II) species are useful complexes as precursors in the hydrogenation of apolar double bonds [18], transfer hydrogenation of polar double bonds [19–21], hydroformylation – hydrogenation, hydroformylation – acetalization [22] and oxidation of alkenes [23,24].

Our group has been studying the various application of *cis*-[$RuCl_2(dppb)(bipy)$] **(1A)** [25], which can be mentioned as an agent with cytotoxic activities [26,27], as an aggregator agent to produce supramolecular species with gold nanoparticles [28–30], as a sensor for electrochemical devices [28,29], as a precursor to prepare polymetallic macrocylics [24], and as a precursor to synthesize vinylidene complexes with photochemical and photophysical properties [31].

Thus, the objective of this study is to optimize the catalytic hydrogenation of cyclohexene by varying bipyridine (bipy) derivatives, replacing the chloride for pseudohalides, evaluating the dependence of the solvent and the pressure in the process. Suitable crystals of *cis*-[Ru(N_3)$_2$(dppb)(bipy)]**(4)**, *cis*-[Ru(CN)$_2$(dppb)(bipy)]**(5)**, *cis*-[Ru(SC$\underline{N}$)$_2$(dppb)(bipy)]**(6),** *cis*-[Ru(CN)$_2$(dppb)(Me-bipy)]**(8)** and *cis*-[Ru(SC$\underline{N}$)$_2$(dppb)(MeO-bipy)]**(11)** were obtained and the X-ray structures are presented here. The X-ray structure of the solvate complex [RuCl(CH_3CN)(dppb)(bipy)](PF_6) (**1B**) was also determined and is presented in the same way.

2. Experimental

2.1. Reagents

All reactions were carried out under argon atmosphere using standard Schlenk techniques. $RuCl_3$ xH_2O, triphenylphosphine (PPh_3), 1,4-bis(diphenylphosphino)butane (dppb), 2,2′-bipyridine (bipy), 4,4′-dimethyl-2,2′-bipyridine (Me-bipy), 4,4′-dimethoxy-2,2′-bipyridine (MeO-bipy), sodium azide (NaN_3), potassium cyanide (KCN), potassium thiocyanate (KSCN) were purchased from Sigma – Aldrich and used as received. Reagent grade solvents were distilled prior to use. The *cis*-[$RuCl_2$(dppb)(bipy)] **(1A)**, *cis*-[$RuCl_2$(dppb)(Me-bipy)] **(2)** and *cis*-[$RuCl_2$(dppb)(MeO-bipy)] **(3)** were prepared as described previously [25].

2.2. Instrumentation

The NMR spectra of the compounds were performed at Federal University of São Carlos, São Carlos (SP). They were acquired using a Bruker DRX-400 spectrometer (9.4 T) equipped with a 5 mm inverse probe head. Samples for $^{31}P\{^1H\}$ experiments were prepared under inert atmosphere and measured at room temperature, with methylene chloride (CH_2Cl_2) as a solvent and a D_2O capillary. Chemical shifts were reported regarding to the phosphorus signal in 85% phosphoric acid (H_3PO_4).

The microanalyses were performed at the Federal University of São Carlos, São Carlos (SP), using a FISONS CHNS-O, mod. EA 1108 Element analyzer.

The FTIR spectra of the powder complexes were recorded from KBr pellets in the 4000 – 200 cm^{-1} range, in a Bomen – Michelson FT MB – 102 instrument.

The UV/Vis spectra of the complexes, in dichloromethane solution, concentration of 1×10^{-3} mol L^{-1}, were recorded using a Hewlett Packard diode array – 8452 A.

Cyclic voltammetry (CV) experiments of the complexes, in solution, were conducted in an electrochemical analyzer BAS model 100B Instrument. These experiments were carried out at room temperature in CH_2Cl_2 or in acetonitrile containing 0.10 mol L^{-1} Bu_4NClO_4 (TBAP) (Fluka Purum) as a support electrolyte using a one-compartment cell, where the working and auxiliary electrodes were stationary Pt foils, and the reference electrode was Ag/AgCl, 0.10 mol L^{-1} TBAP in CH_2Cl_2. Under these conditions, ferrocene was oxidized at 0.43 V (Fc^+/Fc).

Gas chromatography analyses were run on a Shimadzu GC-17A instrument using an Agilent HP-5 column (30 m, 0.32 mm diam., 0.25 μm film); carrier gas; N_2, flow rate; 0.9 mL min^{-1} and hexadecane as an internal standard (1.0×10^{-2} mol L^{-1}).

2.3. X-ray diffraction data

Crystals of *cis*-[Ru(N_3)$_2$(dppb)(bipy)]**(4)**, *cis*-[Ru(CN)$_2$(dppb)(bipy)]**(5)** and *cis*-[Ru(SCN)$_2$(dppb)(bipy)]**(6)** were grown by slow evaporation of a dichloromethane/diethyl ether solution. Meanwhile, crystals of *cis*-[Ru(CN)$_2$(dppb)(Me-bipy)]**(8)** and *cis*-[Ru(SCN)$_2$(dppb)(MeO-bipy)]**(11)** were obtained from slow evaporation of a dichloromethane/methanol solution containing one drop of water. The crystals were mounted on an Enraf-Nonius Kappa-CCD diffractometer with graphite-monochromated MoKα (λ = 0.71073 Å) radiation. The final unit-cell parameters were based on all reflections. Data were collected using the COLLECT program [32] integration and scaling of the reflections were performed with the HKL DENZO-SCALEPACK software package [33]. Absorption corrections were carried out using the Gaussian method [34]. The structures were determined by direct methods with SHELXS-97 [35]. The model was refined by full-matrix least squares on F2 by means of SHELXL-97 [36]. All hydrogen atoms were stereochemically positioned and refined with a riding model. The figures were prepared with ORTEP-3 for Windows [37]. Hydrogen atoms on the aromatic rings were refined isotropically, each one with a thermal parameter 20% greater than the equivalent isotropic displacement parameter of the atom to which it was bonded. The data collection and experimental details are summarized in Table 1S – 5S (see supplementary data), and the selected bond distances and angles are given in **Table 1**.

In the crystal structure of **(1B)**, a methanol molecule exhibited high thermal motions and disorder on the solvation sphere of the complex. The disordered solvent was subtracted from the overall diffraction data following a well-established method called SQUEEZE [38], which showed a total solvent accessible area volume of c.a. 598 Å^3. SQUEEZE calculations indicated the presence of 18e$^-$ per unit cell, which may be attributed to one molecule of methanol present in each unit cell. The structure of **(1B)** is also octahedrally distorted, as observed by the bond angles (see supplementary data), which deviate from the ideal value (90°) in a monoclinic crystal system and P2$_1$/*n* space group (**Table 6S**).

2.4. Preparation of ruthenium (II) complexes

[RuCl(CH_3CN)(dppb)(bipy)](PF_6) (1B): It was synthesized from the *cis*-[RuCl_2(dppb)(bipy)] **(1A)** [25] (80.0 mg, 0.10 mmol) in CH_2Cl_2 (5 mL) with an excess of acetonitrile (31.3 µL, 0.60 mmol). NH_4PF_6 (0.025 mg, 0.16 mmol) was added to the ruthenium solution and then stirred for 24 h under an argon atmosphere. The volume was reduced to approximately 2 mL and diethyl ether (15 mL) was added to precipitate the product, which was filtered off and washed with water (2 x 10 mL) and diethyl ether (2 x 5 mL). Yield 81.5 mg of a yellow powder (90%). Crystals suitable for determining the X-ray structure of the complex were produced from the CH_2Cl_2/Et_2O solution, by slow evaporation. Anal. Calc. for $C_{40}H_{39}N_3ClF_6P_3Ru$: exp. (cal.): C, 53.29 (53.07); H, 4.50 (4.34); N, 4.75 (4.64). Molar conductivity (CH_2Cl_2, 1.0×10^{-3} mol L^{-1}) Λ_m (S cm^{-2} mol^{-1}) 48.2. Cyclic voltammetry (CH_3CN, TBAP 10^{-1} mol L^{-1}): V (Ru^{III}/Ru^{II}): 1.40. IR (cm^{-1}): (ν_{CN}) 2240 (s); ($\nu_{P\text{-}F}$) 557 (s). $^{31}P\{^1H\}$ NMR (162 MHz, CD_3CO, 298 K): δ (ppm) 40.7 (d) and 34.2 (d) $^2J_{PP}$ = 27.1 Hz. UV/Vis (CH_2Cl_2, 2.5×10^{-5} mol L^{-1}): λ/nm (ε/ mol^{-1} L cm^{-1}) 290 (2.2×10^4); 415 (3.9×10^3).

cis-[Ru(L)$_2$(dppb)(N-N)], L = N_3^-, CN$^-$ or SCN$^-$, N-N = bipy, Me-bipy or MeO-bipy

A typical experiment to prepare the pseudohalide complexes containing ruthenium II **(4)** – **(11)**, with general formula *cis*-[Ru(L)$_2$(dppb)(N-N)] is described as follows for *cis*-[Ru(N_3)$_2$(dppb)(bipy)]**(4)**: the precursor *cis*-[RuCl_2(dppb)(bipy)] **(1A)** [25] (42.0 mg, 0.055 mmol) was dissolved in the presence of NaN_3 (11.0 mg, 0.165 mmol) in a mixture of CH_2Cl_2/methanol (1:1). The reaction mixture was stirred under Ar atmosphere for 24 h. The final red solution was concentrated to ca. 5 mL and 10 mL of diethyl ether was added to obtain a dark red precipitate, which was filtered off, washed with water and dried under vacuum. Yield 40 mg of a red powder (96 %). Anal. Calc. for $C_{38}H_{36}N_8P_2Ru.CH_3OH$: exp. (cal.): C, 58.91 (58.57); H, 4.89 (5.04); N, 14.40

(14.01). Molar conductivity (CH_2Cl_2, 1.0 × 10^{-3} mol L^{-1}) Λ_m (µS cm^{-1}) 2.25. Cyclic voltammetry (CH_3CN, TBAP 10^{-1} mol L^{-1}): V (Ru^{III}/Ru^{II}): 0.55. IR (cm^{-1}): (ν_{asNNN}) 2040 (s); (ν_{sNNN}) 1436 (w); (δ_{-NNN}) 693 (w); ($\nu_{Ru\text{-}NNN}$) 431 / 409 (w). $^{31}P\{^1H\}$ NMR (162 MHz, $CDCl_3$, 298 K): δ (ppm) 38.7 (d) and 38.1 (d) $^2J_{PP}$ = 32.8 Hz. UV/Vis (CH_2Cl_2, 10^{-5} mol L^{-1}): λ/nm (ε/ mol^{-1} L cm^{-1}) 308 (1.8 × 10^4); 338 (5.0 × 10^3); 469 (2.3 × 10^3).

***cis*-[Ru(CN)$_2$(dppb)(bipy)]** (**5**): KCN (10.0 mg, 0,165 mmol) and *cis*-[$RuCl_2$(dppb)(bipy)] **(1A)** [25](42.0 mg, 0.055 mmol). Yield 38 mg of a yellow powder (94%). Anal. Calc. $C_{40}H_{36}N_4P_2Ru_,$ exp. (cal.); C, 65.20 (65.30); H, 4.75 (4.93); N, 7.31 (7.61). Molar conductivity (CH_2Cl_2, 1.0 × 10^{-3} mol L^{-1}) Λ_m (µS cm^{-1}) 2.25. Cyclic voltammetry (CH_3CN, TBAP 10^{-1} mol L^{-1}): V (Ru^{III}/Ru^{II}): 1.16. IR (cm^{-1}): (ν_{CN}) 2091/2072 (s); ($\nu_{Ru\text{-}CN}$) 427/416 (w); ($\nu_{Ru\text{-}P}$) 502 (m); $\nu_{(Ru\text{-}N)}$ 455 (w). $^{31}P\{^1H\}$ NMR (162 MHz, $CDCl_3$, 298 K): δ (ppm) 45.8 (d) and 25.2 (d) $^2J_{PP}$ = 23.4Hz. UV/Vis (CH_2Cl_2, 10^{-5} mol L^{-1}): λ/nm (ε/ mol^{-1} L cm^{-1}) 303 (2,0 × 10^4); 412 (4.2 × 10^3).

***cis*-[Ru(SC$\underline{N}$)$_2$(dppb)(bipy)]** (**6**): KSCN (16.0 mg, 0,165 mmol) and *cis*-[$RuCl_2$(dppb)(bipy)] **(1A)** [25] (42.0 mg, 0.055 mmol). Yield 41 mg of a yellow powder (94%). Anal. Calc. $C_{40}H_{36}N_4P_2RuS_2$ exp. (cal.); C, 60.27 (60.06); H, 4.67 (4.53); N, 6.73 (7.00); S, 8.21 (7.67). Molar conductivity (CH_2Cl_2, 1.0 × 10^{-3} mol L^{-1}) Λ_m (µS cm^{-1}) 2.46. IR (cm^{-1}): (ν_{CN}) 2113/2103 (s); (ν_{CS}) 762/740 (w); (δ_{NCS}) 431. Cyclic voltammetry (CH_3CN, TBAP 10^{-1} mol L^{-1}): V (Ru^{III}/Ru^{II}): 0,73. $^{31}P\{^1H\}$ NMR (162 MHz, $CDCl_3$, 298 K): δ (ppm) 40.4 (d) and 35.9 (d) $^2J_{PP}$ = 32 Hz. UV/Vis (CH_2Cl_2, 10^{-5} mol L^{-1}): λ/nm (ε/ mol^{-1} L cm^{-1}) 307 (2.2 × 10^4); 447 (3.9 × 10^3); 492 (2.4 × 10^3).

***cis*-[Ru(N$_3$)$_2$(dppb)(Me-bipy)]** (**7**): NaN_3 (11.0 mg, 0,165 mmol) and *cis*-[$RuCl_2$(dppb)(Me-bipy)] **(2)** [25] (43.0 mg, 0.055 mmol). Yield 42 mg of a red powder (96%). Anal. Calc. $C_{40}H_{40}N_8P_2Ru$: exp. (cal.); C, 59.89 (60.37); H, 5.05 (5.07); N, 14.12 (14.08). Molar conductivity (CH_2Cl_2, 1.0×10^{-3} mol L^{-1}) Λ_m (μS cm^{-1}) 2.46. IR (cm^{-1}): (ν_{asNNN}) 2037 (s); (ν_{sNNN}) 1431 (w); (δ_{NNN}) 696 (w); ($\nu_{Ru\text{-}NNN}$) 435/412 (w). Cyclic voltammetry (CH_3CN, TBAP 10^{-1} mol L^{-1}): V (Ru^{III}/Ru^{II}): 0.46. $^{31}P\{^1H\}$ NMR (162 MHz, $CDCl_3$, 298 K): δ (ppm) 38.7 (d) and 37.2 (d) $^2J_{PP}$ = 32 Hz. UV/Vis (CH_2Cl_2, 10^{-5} mol L^{-1}): λ/nm (ε/ mol^{-1} L cm^{-1}) 307 (2.1×10^4); 338 (9.8×10^3); 457 (5.0×10^3).

***cis*-[Ru(CN)$_2$(dppb)(Me-bipy)] (8)**: KCN (10.0 mg, 0,165 mmol) and *cis*-[$RuCl_2$(dppb)(Me-bipy)] **(2)** [25] (45.0 mg, 0.055 mmol). Yield 39 mg of a yellow powder (94%). Anal. Calc. $C_{42}H_{40}N_4P_2Ru$: exp. (cal.); C, 66.09 (66.04); H, 5.12 (5.27); N, 7.21 (7.33). Molar conductivity (CH_2Cl_2, 1.0×10^{-3} mol L^{-1}) Λ_m (μS cm^{-1}) 2.46. Cyclic voltammetry (CH_3CN, TBAP 10^{-1} mol L^{-1}): V (Ru^{III}/Ru^{II}): 1.40. IR (cm^{-1}): (ν_{CN}) 2091/2066 (s); ($\nu_{Ru\text{-}CN}$) 427/408 (w); ($\nu_{Ru\text{-}P}$) 495 (m); $\nu_{(Ru\text{-}N)}$ 444 (w). $^{31}P\{^1H\}$ NMR (162 MHz, $CDCl_3$, 298 K): δ (ppm) 46 (d) and 25.9 (d) $^2J_{PP}$ = 24 Hz. UV/Vis (CH_2Cl_2, 10^{-5} mol L^{-1}): λ/nm (ε/ mol^{-1} L cm^{-1}) 303 ($2,0 \times 10^4$); 407 (4.4×10^3).

***cis*-[Ru(N$_3$)$_2$(dppb)(MeO-bipy)] (9)**: NaN_3 (11.0 mg, 0,165 mmol) and *cis*-[$RuCl_2$(dppb)(MeO-bipy)] **(3)** [25] (45.0 mg, 0.055 mmol). Yield 44 mg of a red powder (94%). Anal. Calc. $C_{40}H_{40}N_8O_2P_2Ru$: exp. (cal.); C, 58.12 (58.04); H, 4.94 (4.87); N, 13.63 (13.54). Molar conductivity (CH_2Cl_2, 1.0×10^{-3} mol L^{-1}) Λ_m (μS cm^{-1}) 1.96. IR (cm^{-1}): (ν_{asNNN}) 2038 (s); (ν_{sNNN}) 1434/1414; (δ_{NNN}) 710 (w); ($\nu_{Ru\text{-}NNN}$) 415/438 (w). Cyclic voltammetry (CH_3CN, TBAP 10^{-1} mol L^{-1}): V (Ru^{III}/Ru^{II}): 0.46. $^{31}P\{^1H\}$ NMR (162 MHz, $CDCl_3$, 298 K): δ (ppm) 40.8 (d) and 37.8 (d) $^2J_{PP}$ = 32 Hz. UV/Vis (CH_2Cl_2, 10^{-5} mol L^{-1}): λ/nm (ε/ mol^{-1} L cm^{-1}) 302 (2.1×10^4); 332 (9.4×10^3); 435 (5.0×10^3).

***cis*-[Ru(CN)$_2$(dppb)(MeO-bipy)] (10)**: KCN (10.0 mg, 0,165 mmol) and *cis*-[RuCl$_2$(dppb)(MeO-bipy)] **(3)** [25] (43.0 mg, 0.055 mmol). Yield 41 mg of a yellow powder (94%). Anal. Calc. $C_{42}H_{40}N_4O_2P_2Ru$: exp. (cal.); C, 63.29 (63.38); H, 5.12 (5.07); N, 6.98 (7.04). Molar conductivity (CH_2Cl_2, 1.0×10^{-3} mol L^{-1}) Λ_m (μS cm^{-1}) 1.96. IR (cm^{-1}): (ν_{CN}) 2097 (s); ($\nu_{Ru\text{-}CN}$) 424/415 (w); ($\nu_{Ru\text{-}P}$) 494 (m); ($\nu_{Ru\text{-}N}$) 449 (w). Cyclic voltammetry (CH_3CN, TBAP 10^{-1} mol L^{-1}): V (Ru^{III}/Ru^{II}): 1.34. $^{31}P\{^1H\}$ NMR (162 MHz, $CDCl_3$, 298 K): δ (ppm) 46.0 (d) and 25.6 (d) $^2J_{PP}$ = 23.9 Hz. UV/Vis (CH_2Cl_2, 10^{-5} mol L^{-1}): λ/nm (ε/ mol^{-1} L cm^{-1}) 302 (2.1×10^4); 332 (9.4×10^3); 435 (5.0×10^3).

***cis*-[Ru(SC$\underline{N}$)$_2$(dppb)(MeO-bipy)] (11)**: KSCN (16.0 mg, 0,165 mmol) and *cis*-[RuCl$_2$(dppb)(MeO-bipy)] **(3)** [25] (42.0 mg, 0.055 mmol). Yield 41 mg of a yellow powder (94%). Anal. Calc. $C_{42}H_{40}N_4O_2P_2RuS_2$:exp. (cal.); C, 58.41 (58.66); H, 4.75 (4.69); N, 6.31 (6.51); S, 8.01 (7.30). Molar conductivity (CH_2Cl_2, 1.0×10^{-3} mol L^{-1}) Λ_m (μS cm^{-1}) 1.96. IR (cm^{-1}): (ν_{CN}) 2112/2106 (s); (ν_{CS}) 700/689 (w); (δ_{NCS}) 435. Cyclic voltammetry (CH_3CN, TBAP 10^{-1} mol L^{-1}): V (Ru^{III}/Ru^{II}): 0,89. $^{31}P\{^1H\}$ NMR (162 MHz, $CDCl_3$, 298 K): δ (ppm) 43 (d) and 36.5(d) $^2J_{PP}$ = 31.8 Hz. UV/Vis (CH_2Cl_2, 10^{-5} mol L^{-1}): λ/nm (ε/ mol^{-1} L cm^{-1}) 307 (2.3×10^4); 446 (4.0×10^3); 487 (2.5×10^3).

2.5. Hydrogenation of cyclohexene

Hydrogenation reactions were carried out in a stainless-steel autoclave Paar – Model 4842 with a volume capacity of 100 cm^3 equipped with an overhead magnetic stirrer, a digital pressure indicator and a thermocouple to record temperature. The autoclave was equipped with an electrical heating/cooling system to control the temperature inside the vessel. In a typical reaction, the catalyst precursor (ruthenium complexes from **(1)** to **(11)**, (7.0×10^{-3} mmol) was dissolved in 20 mL of the appropriate solvent (isopropanol, methanol, ethanol, dimethylsulphoxide, dichloromethane, acetonitrile or acetone) inside the autoclave in the presence of cyclohexene (7.0 mmol) under Ar atmosphere. After that, the autoclave was flushed out threefold with molecular hydrogen (H_2), then the autoclave was pressurized with H_2 (within 1 to 20 atm) and heated to a temperature of 25 – 80 °C, for 1 – 24 h. After the reaction, the homogeneous reaction mixture was cooled down in an ice bath to room temperature and the upper organic layer was analyzed by gas chromatography (GC-FID). Hexadecane (1.0×10^{-2} mol L^{-1}) was used as an internal standard.

3. Results and discussion

3.1. Characterization of ruthenium complexes

The Ruthenium complexes *cis*-[Ru(L)$_2$(dppb)(N-N)] {where L = N_3^-, CN^- and SCN^-, N-N = bipy, Me-bipy and MeO-bipy} were prepared by chloride exchange on the *cis*-[RuCl$_2$(dppb)(N-N)] complexes in a mixture of CH_2Cl_2:MeOH (1:1) (see Scheme 1). These compounds were characterized by spectroscopic and electrochemical techniques, by elemental analyses, as well as by molar conductance. Moreover, they are compatible with expectations for (**4**) - (**11**) complexes, suggesting the presence of neutral compounds.

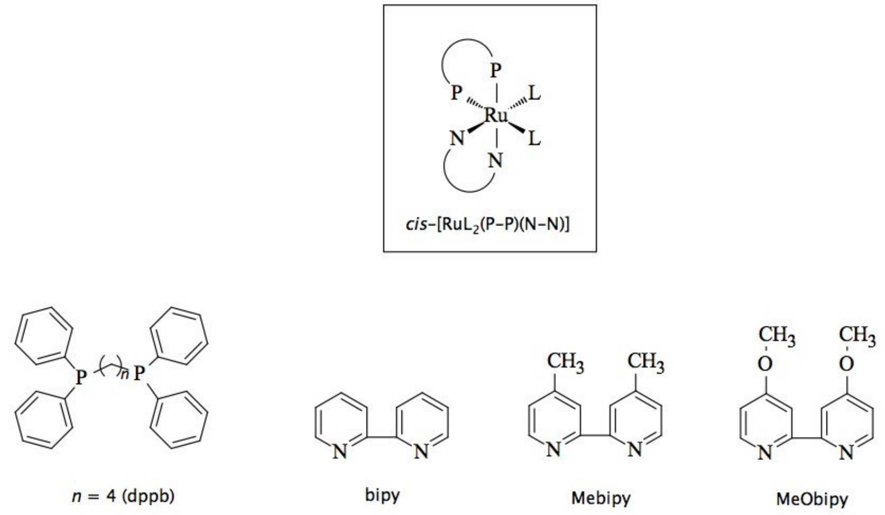

Complex	P – Donor Group	N – Donor Group	L – Donor Group
(1)	dppb	bipy	Cl^-
(2)	dppb	Mebipy	Cl^-
(3)	dppb	MeObipy	Cl^-
(4)	dppb	bipy	N_3^-
(5)	dppb	bipy	CN^-
(6)	dppb	bipy	SCN^-
(7)	dppb	Mebipy	N_3^-
(8)	dppb	Mebipy	CN^-
(9)	dppb	MeObipy	N_3^-
(10)	dppb	MeObipy	CN^-
(11)	dppb	MeObipy	SCN^-

Scheme 1: General structure and numerical label of the ruthenium complexes [39].

The solvate complex [RuCl(CH$_3$CN)(dppb)(bipy)]PF$_6$ **(1B)** was formed in presence of an excess of CH$_3$CN in CH$_2$Cl$_2$ solution of the *cis*-[RuCl$_2$(dppb)(bipy)] **(1A)**. The X-ray structure of **(1B)** was determined and its structure is depicted in **Fig. 1**. The structure is octahedral distorted, with the acetonitrile *trans* to N atom from the bipy ligand. Additionally, the starting complex **(1A)** can provide a solvate complex in the presence of methanol, but in this case the methanol molecule coordinates in the *trans* position to phosphorus P atom of the dppb ligand. The X-ray structure of the complex [RuCl(CH$_3$OH)(dppb)(bipy)](PF$_6$) **(1C)** was determined in an octahedral distorted environment such as previously published [30]. Crystal data and structure refinement parameters for complex **(1B)** can be found in the supplementary material (**Table 6S**).

The crystals structures of complexes (**4**), **(5), (6), (8)** and **(11)** determined from single-crystal X-ray diffraction are also shown in **Fig. 1**. Different from the case to obtain **(1B)** and **(1C)**, the two Cl^- ligands present in the precursor **(1A)** were exchanged for two pseudohalides and the *cis* configuration was maintained in all complexes. Selected bond lengths and angles are listed in **Table 1**. Crystal data and structure refinement of complexes (**4**), **(5)**, **(6)**, **(8)** and **(11)** are described in the supplementary material **(Tables 1S – 5S)**.

The structures are octahedral distorted, as observed by the bond angles, which deviate from the ideal value (90°), mainly in the N_{bipy}–Ru–N_{bipy} angle forming a five-membered chelating ring. The Ru–P distances *trans* to pseudohalides are 2.2907(9), 2.4012(8), 2.3321(9), 2.3930(15) and 2.3234(9) Å for the complexes (**4**), (**5**), (**6**), (**8**) and (**11**), respectively. These values are larger than those observed for the Ru–P bond *trans* to Cl^- ligand in *cis*-[$RuCl_2$(dppb)(bipy)] complex (2.279(3) A˚) [25]. Similarly, the Ru–N (bipyridine) bond length for the ruthenium dichloride complex is shorter than those observed for the five complexes reported here. These data are consistent with the substitution of Cl^- ligand, a good σ and π donor by an π-acceptor ligand and can be explained by the backbonding interaction involving the pseudohalide ligand and Ru (II), as suggested by Brito et al [40].

Table 1: Selected bond lengths and angles of the crystal structures of the complexes **(4)**, **(5)**, **(6)**, **(8)** and **(11)**.

	Complex				
Bond lengths (Å)	**(4)**	**(5)**	**(6)**	**(8)**	**(11)**
P-Ru *trans* L	2.2907(9)	2.4006(8)	2.3321(9)	2.3930(15)	2.3234 (9)
P-Ru *trans* bipy	2.3151(8)	2.2993(9)	2.3462(10)	2.2951(13)	2.3216(11)
N$_{bipy}$-Ru *trans* L	2.085(2)	2.171(2)	2.106(2)	2.178(4)	2.118 (2)
N$_{bipy}$-Ru *trans* P	2.3151(8)	2.132(3)	2.121(3)	2.133(4)	2.132(2)
L-Ru *trans* P	2.173(3)	2.030(3)	2.110(3)	2.040(6)	2.102 (2)
L-Ru *trans* N$_{bipy}$	2.111(3)	1.986(3)	2.070(3)	1.987(6)	2.048(3)
N(1)-N(2)	1.182(3)				
N(2)-N(3)	1.162(4)				
N(4)-N(5)	1.182(4)				
N(5)-N(6)	1.162(4)				
N(1)-C(1)		1.156(4)	1.144(4)	1.15(1)	1.150 (3)
N(2)-C(2)		1.152(4)	1.138(4)	1.154(8)	1.159(4)
S(1)-C(1)			1.626(3)		1.631(3)
S(2)-C(2)			1.633(4)		1.619(4)
Bond angles (°)					
P-Ru-P	94.20(3)	93.00(3)	94.33(3)	93.43(5)	94.42(3)
N$_{bipy}$-Ru-N$_{bipy}$	77.89(9)	76.10(10)	76.93(11)	75.81(16)	76.78 (9)
L-Ru-L	87.95(10)	92.11(12)	91.56(10)	91.6(2)	95.16(10)
Ru(1)-N(1)-N(2)	123.5(2)				
Ru(1)-N(4)-(5)	133.9(2)				
Ru(1)-C(1)-N(1)		174.8(3)		175.9(6)	
Ru(1)-C(2)-N(2)		175.9(3)		172.9(6)	
Ru(1)-N(1)-C(1)			165.5(3)		164.9(2)
Ru(1)-N(2)-C(2)			162.7(3)		160.4(3)
N(1)-C(1)-S(1)			178.5(3)		179.2(3)
N(2)-C(2)-S(2)			178.6(3)		176.6(3)

L = pseudohalide N_3^-, CN^- or SC$\underline{N}^-$. **(4)** = *cis*-[Ru(N_3)$_2$(dppb)(bipy)], **(5)** = *cis*-[Ru(CN)$_2$(dppb)(bipy)], **(6)** = *cis*-[Ru(SC$\underline{N}$)$_2$(dppb)(bipy)], **(8)** = *cis*-[Ru(CN)$_2$(dppb)(Mebipy)], **(11)** = *cis*-[Ru(SC$\underline{N}$)$_2$(dppb)(MeObipy)].

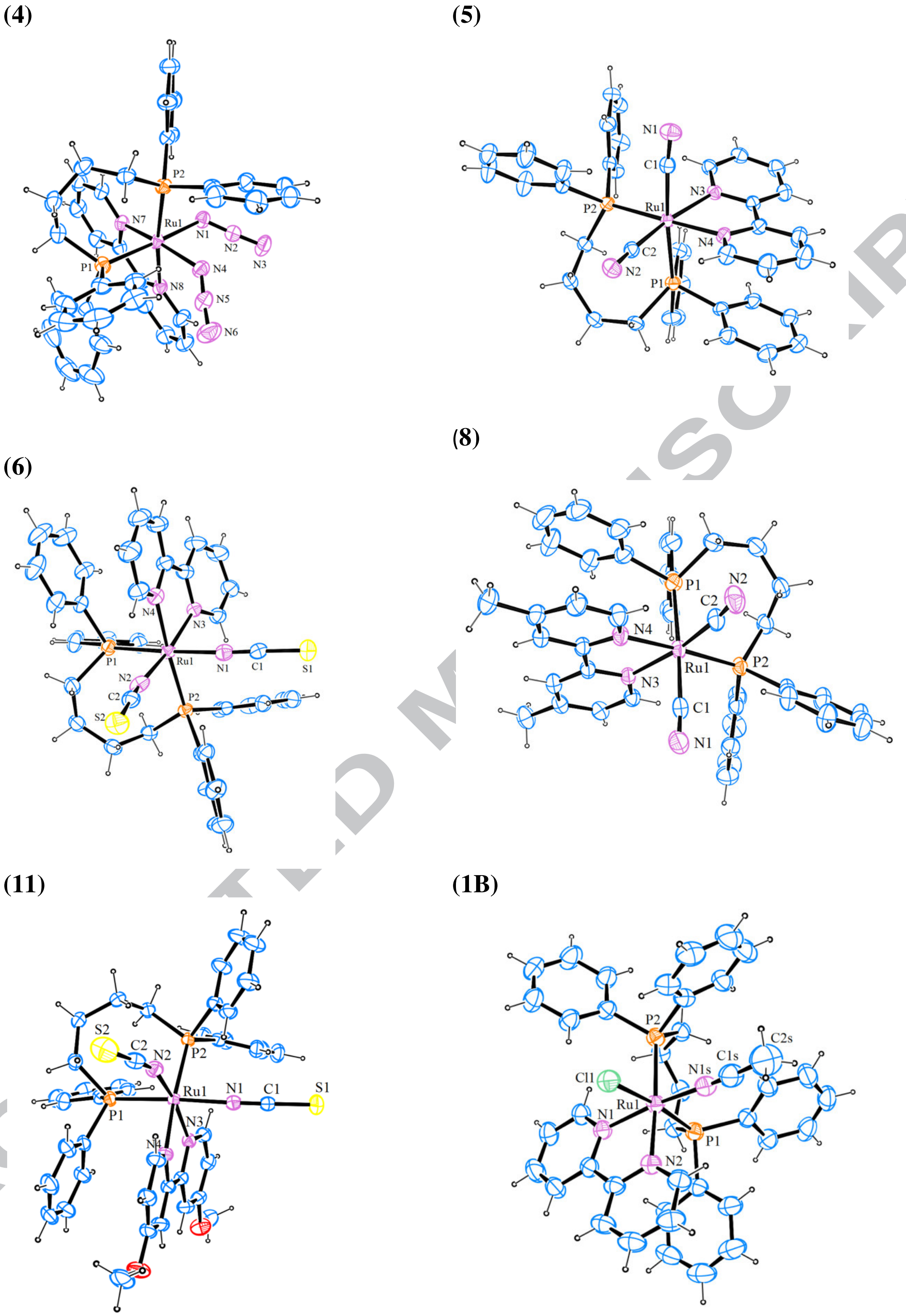
(4) (5) (6) (8) (11) (1B)

Fig. 1: ORTEP [37] view of the crystal structures showing main atoms labeling and 30% of probability ellipsoids. *cis*-[Ru(N_3)$_2$(dppb)(bipy)] **(4)** *cis*-[Ru(CN)$_2$(dppb)(bipy)] **(5)** *cis*-[Ru(SC<u>N</u>)$_2$(dppb)(bipy)] **(6)** *cis*-[Ru(CN)$_2$(dppb)(Mebipy)] **(8)** *cis*-[Ru(SC<u>N</u>)$_2$(dppb)(MeObipy)] **(11)**, and [RuCl(CH_3CN)(dppb)(bipy)]$^+$ (**1B**).

As depicted in **Table 1**, the 4-substituted position in the bipyridine rings with the methyl or methoxy group does not have an effective electronic influence on the Ru−L bond length {L = pseudohalide N_3^-, CN^- or $SC\underline{N}^-$}. A bond length of 1.98 Å was observed for the Ru−CN bond in complex **(5)**, which has a CN^- group *trans* to the nitrogen of the bipy ligand, while complex **(8)** has a CN^- group *trans* to the nitrogen of the Me-bipy ligand. Similar behavior was detected for complexes **(6)** and **(11)**, where the Ru−NCS^- bond lengths of 2.070(3) and 2.048(3), were observed respectively.

Two different angles were observed in the Ru-N_3 bonds in the crystal structure of the complex **(4)**, where the angles between the bonds Ru(1)-N(1)-N(2) and Ru(1)-N(4)-(5) are 123.5(2)° and 133.9(2)°, respectively. These results can have two different explanations. The first one is suggested to be a consequence of the steric hindrance of the aromatic rings of the dppb over the N_3^-. The second one finds support in the molecular orbital of the N_3^- molecule. The bonds in the free N_3^-, with a linear shape, have the same length, 1.16 Å. However, the HN_3 molecule has a bent structure, where the bond angle H–N–N is 112° [41]. This means that the extra electron from H must occupy an antibonding molecular orbital, providing N–N bonds with significantly different lengths, i.e. 1.24 Å and 1.13 Å. The bond orders are presumably 1.5 and 2 respectively [41]. The N–N–N bond lengths found in complex **(4)** fits well with what was described above for the HN_3 molecule. The N(1)-N(2) and N(4)-N(5) bonds, which are closer to the metal center, have bond lengths of 1.182(3) Å and 1.182(4) Å respectively, while bonds N(2)-N(3) and N(5)-N(6) are slightly shorter, 1.162(4) Å and 1.162(4) Å, respectively. These results also indicate different bond orders in the bonds of the N_3^- coordinated to ruthenium.

As the bond angle Ru–N–N in complex **(4)** is greater than H–N–N in the HN_3 molecule, it is reasonable to think that the N_3^- is a weak π-acceptor, when it is compared with the CN⁻ and SC<u>N</u>⁻. The bond angles Ru(1)-C(1)-N(1) in **(8)**, and Ru(1)-N(1)-C(1) in **(6)** are 175.9° and 165.5°, respectively. These results indicate a double bond character between ruthenium-CN⁻ and ruthenium- SC<u>N</u>⁻ ligands. Hence, a descending order of π-acceptor electron density of the pseudohalide groups can be described as follows: $CN^- > SC\underline{N}^- > N_3^-$. This series is the same observed in the $^{31}P\{^1H\}$ NMR data as described below, and it agrees with the spectrochemical series found in the literature on inorganic chemistry [42].

The pseudohalide ligands present a strong band at FTIR spectra in the region around 2000 cm^{-1}. The FTIR spectra of c*is*-$[Ru(CN)_2(dppb)(bipy)]$**(5)**, c*is*-$[Ru(CN)_2(dppb)(Mebipy)]$**(8)** and c*is*-$[Ru(CN)_2(dppb)(MeObipy)]$**(10)** show two well-defined bands around 2090 and 2065 cm^{-1}, due to the symmetric and antisymmetric stretching mode combinations of the CN⁻, while only one band was observed in the *cis*-$[Ru(N_3)_2(dppb)(bipy)]$**(4)** and *cis*-$[Ru(SC\underline{N})_2(dppb)(bipy)]$**(6)** complexes [43,44]. The FTIR spectra of *cis*-$[Ru(SC\underline{N})_2(dppb)(bipy)]$**(6)** and *cis*-$[Ru(SC\underline{N})_2(dppb)(MeObipy)]$**(11)** present a N=C stretching peak around 2100 cm^{-1} [45,46]. The *cis*-$[Ru(N_3)_2(dppb)(bipy)]$ complex also revealed a single band near to 2000 cm^{-1}, due to the antisymmetric stretching mode of the N_3^-, as previously reported for the similar complex, $[Ru(N_3)_2(bipy)_2]$ [47].

The pseudohalide complexes **(4)** – **(11)** were dissolved in CH_2Cl_2 (1.0×10^{-5} mol L^{-1}) and their electronic spectra at ultraviolet/visible region (UV/vis) were recorded, which reveal two distinct bands. The higher energy bands are assigned to the N-N and P-P donor groups, which present an electronic transition between molecular orbitals, located in the ligands (π→π*), more appropriately known as an intraligand transition (IL). The lower energy bands are assigned to the metal-ligand charge transfer (MLCT), which occurs in the visible region, corresponding to an electronic transition from a metal based dπ orbital to a bipy ligand-based orbital π^* [48–50]. **Table 2** summarizes the results observed in the UV/vis spectra of the complexes **(4)** – **(11)**.

Table 2: UV/vis data for the *cis*-[Ru(X)$_2$(dppb)(N-N)] complexes in CH_2Cl_2 (1.0×10^{-5} mol L^{-1}).

Complex	**λ (nm) $\pi \rightarrow \pi^*$ ($\times 10^4$ ε L mol^{-1} cm^{-1})**	**λ (nm) d$\pi_{(Ru)} \rightarrow \pi^*$ ($\times 10^3$ ε L mol^{-1} cm^{-1})**
(4)	308 (1.8)	469 (2.3)
(5)	303 (2.0)	412 (4.2)
(6)	307 (2.2)	447 (3.9), 492 (2.4)
(7)	307 (2.1)	435 (5.0)
(8)	304 (2.2)	412 (4.8)
(9)	302 (2.1)	435 (5.0)
(10)	303 (2.0)	407 (4.4)
(11)	307 (2.3)	446 (4.0), 487 (2.5)

The voltammetry studies for the complexes (**4**), **(7)** and **(9)** present an irreversible process corresponding to the Ru^{III}/Ru^{II} couple with an anodic peak potential (E_{pa}) at 0.55 V for **(4)** and 0.46 for **(7)** and **(9)** (see **Table 3**). This shift to a cathodic region in the cyclic voltammogram, when compared with the precursor *cis*-[RuCl$_2$(dppb)(bipy)] (E_{pa} = 0.7 V) can be attributed to the fact that the N_3^- is a stronger σ-donor ligand than Cl^- and it is a weak π-acceptor. In this case, there is an enrichment of the electronic density in the metal center, which facilitates its oxidation process, providing lower E_{pa}. The second oxidation process observed for complexes (**4**), **(7)** and **(9)** at more anodic potentials (ca. 0.9 V), can be assigned to the oxidation of the N_3^- ligand. The oxidation potential of the free N_3^- ligand, in acetonitrile as a solvent, occurs at 0.79 mV [43]. Complexes (**4**), **(7)** and **(9)** present a third electrochemical process at about 1.2 V, which can be assigned to the Ru^{III}/Ru^{II} process belonging to the [Ru(N$_3$)(CH$_3$CN)(dppb)(N-N)]$^+$ species, which was generated in an acetonitrile solution. The cyclic and differential pulse voltammograms for the [Ru(N$_3$)$_2$(dppb)(bipy)] can be found in the supplementary data (**Fig. 1S**).

Table 3: Cyclic voltammetry parameters to the complexes **(4)** – **(11)**.

Complex	$E_{½}$ (E, mV)^{a}	E_{pa} (V) N_3^-	*E_{pa} (V) $N_3^{-\,b}$
(4)	--- (550)^{c}	0.93	1.32
(5)	1.30 (280)	---	---
(6)	0.84(230)	---	---
(7)	--- (460)^{c}	0.89	1.19
(8)	1.29 (210)	---	---
(9)	--- (460)^{c}	0.90	1.26
(10)	1.26 (150)	---	---
(11)	0.80 (180)	---	---

a) $E_{1/2}$ = half-wave potential (E_{pa}-E_{pc}/2); E = E_{pa}-E_{pc}, where E_{pa} = anodic peak potential, E_{pc} = cathodic peak potential. b) *E_{pa} related to the $[Ru(N_3)(CH_3CN)(dppb)(N\text{-}N)]^+$ complex generated in acetonitrile solution in the CV experiment. c) E = E_{pa} irreversible process. Complexes: **(4)** = *cis*-$[Ru(N_3)_2(dppb)(bipy)]$, **(5)** = *cis*-$[Ru(CN)_2(dppb)(bipy)]$, **(6)** = *cis*-$[Ru(SC\underline{N})_2(dppb)(bipy)]$, **(7)** = *cis*-$[Ru(N_3)_2(dppb)(Mebipy)]$, **(8)** = *cis*-$[Ru(CN)_2(dppb)(Mebipy)]$, **(9)** = *cis*-$[Ru(N_3)_2(dppb)(MeObipy)]$, **(10)** = *cis*-$[Ru(CN)_2(dppb)(MeObipy)]$ and **(11)** = *cis*-$[Ru(SC\underline{N})_2(dppb)(MeObipy)]$.

Cyclic voltammetry of **(5)**, **(6)**, **(8)**, **(10)** and **(11)** showed only one reversible process, corresponding to the Ru^{II}/Ru^{III} couple, with half-wave potential ($E_{1/2}$) values between 0.80 – 1.30 (see **Table 3**). These values are considerable higher than the $E_{1/2}$ normally observed in the dichloride ruthenium complexes with either *trans* or *cis*-$[RuCl_2(P\text{-}P)(N\text{-}N)]$ {where: P-P= biphosphine and N-N=diimines} configuration, which shows $E_{1/2}$ values at around 0.60V [25]. This shift to an anodic region in the cyclic voltammograms can be attributed to the presence of strong π-acceptor ligands, such as CN^- and NCS^-.

The $^{31}P\{^1H\}$ NMR spectra of the complexes **(4)** – **(11)**, in CH_2Cl_2/D_2O, exhibit two doublets, as expected, due to the non-equivalence of phosphorus atoms from the dppb ligand in the *cis* geometry of the complexes. It can be observed in **Table 4** that complexes **(5)**, **(8)** and **(10)** present a doublet signal much more shielded than the correlate complexes with N_3^- and SCN^- ligands. This behavior provides a large variation of the chemical shifts, between the doublets, labeled as Δδ (ppm) (see **Fig. 2**). The presence of a π-acceptor group (CN^-) decreases the back donation towards the phosphorus atoms. Therefore, the Δδ value is around 20 ppm in the presence of CN^- ligand, while in the presence of a weak π-acceptor, such as N_3^- ligand, the Δδ is much lower, less than 3.0 ppm. This result is in agreement with the bond distance observed by X-ray diffraction data, where the more shielded phosphorus atom provides a greater Ru-P bond length.

Table 4: $^{31}P\{^1H\}$ NMR data of the complexes **(4)** – **(11)**.

Complex	**δ $^{31}P\{^1H\}$ (ppm); $^2J_{PP}$ (Hz)**	**Δδ (ppm)**
(4)	38.7, 38.1; 32.8	0.6
(5)	45.8, 25.2; 23.4	20.6
(6)	40.4, 35.9; 31.95	4.5
(7)	38.7, 37.2; 31.9	1.5
(8)	46.0, 25.9; 24.0	20.1
(9)	40.8, 37.8; 32.4	3.0
(10)	46.0, 25.6; 23.9	20.4
(11)	43.0, 36.5; 31.8	6.5

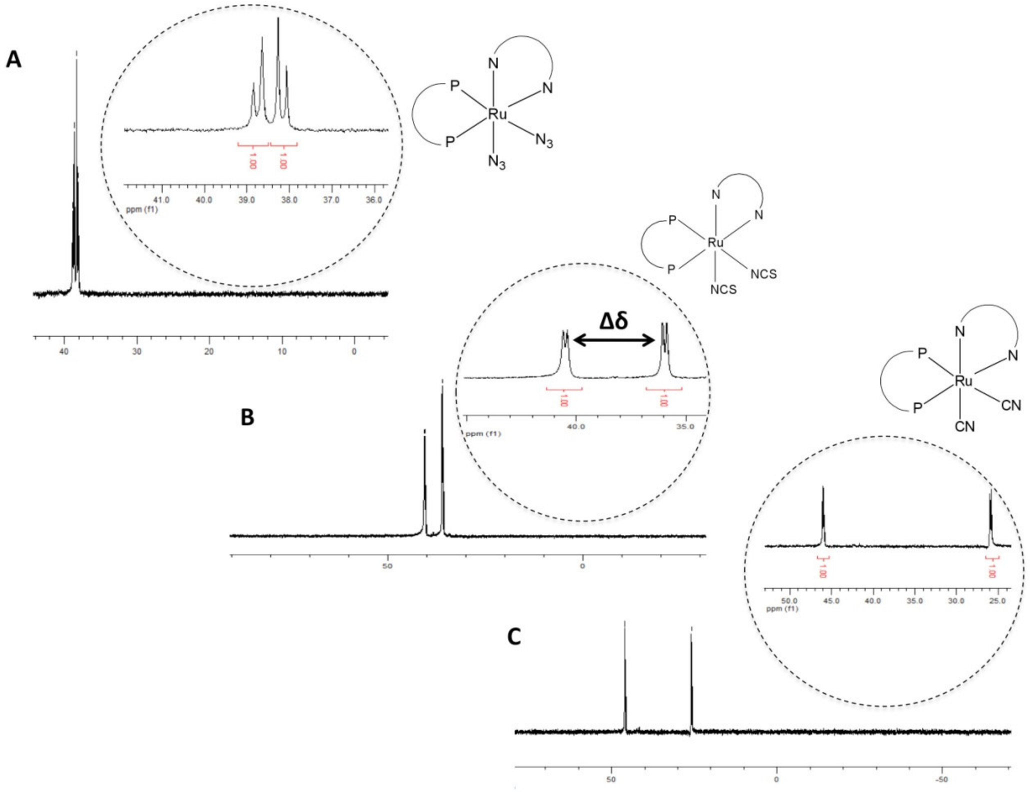

Fig. 2: $^{31}P\{^1H\}$ NMR data of pseudohalide complexes containing ruthenium in CH_2Cl_2/D_2O solution. A) *cis*-[Ru(N_3)$_2$(dppb)(bipy)] **(4)**. B) *cis*-[Ru(CN)$_2$(dppb)(bipy)] **(5)**. C) *cis*-[Ru(SC<u>N</u>)$_2$(dppb)(bipy)] **(6)**. The dashed circle is the amplified spectrum of each complex.

3.2. Hydrogenation of cyclohexene

Hydrogenation reactions of cyclohexene to produce cyclohexane were firstly carried out in the presence of the dichloride complex containing ruthenium, *cis*-[RuCl$_2$(dppb)(bipy)] **(1A)**, in different solvents, pressure of H$_2$, temperature, time and molar ratio between the components. A series of reactions was performed in different solvents to find a better homogeneous condition with a good yield of the saturated product (see **Table 5**).

Table 5: Influence of the solvent on the hydrogenation of cyclohexene catalyzed by *cis*-[RuCl$_2$(dppb)(bipy)]^a (**1**).

Entry	**Solvent**	**% of cyclohexane** ^{a} **± RSD(%)**^{b}	**TOF (h^{-1})**^{c}
1	Isopropanol	87 ± 2	18.13
2	Methanol	99 ± 1	20.83
3	Ethanol	78 ± 5	16.25
4	Dimethyl sulfoxide	4 ± 1	< 1.00
5	Dichloromethane	67 ± 8	13.96
6	Acetonitrile	3 ± 2	< 1.00
7	Acetone	64 ± 6	13.33

Cyclohexene/(**1**) molar ratio = 500, at 25°C, within 24 h and 15 atm of H$_2$. a) Determined by GC analyses. b) Reactions were carried out in threefold analysis, RSD = relative standard deviation. c) TOF (h^{-1}) = turnover frequency = $n_{\text{prod}}/(n_{\text{cat}} \times t)$; where n_{prod} = mol number of product, n_{cat} = mol number of pre-catalyst and t = reaction time (h).

The results showed that 100 % of the hydrogenated product was obtained in methanol (entry 2,**Table 5**), while in the presence of coordinating solvents, such as dimethyl sulfoxide and acetonitrile, the yield of the product drastically decreased. In the presence of other solvents, such as CH$_2$Cl$_2$ or acetone, the amount of hydrogenated product was less satisfactory, but it was still obtained with a good yield, at an average of 65%.

Additionally, the hydrogenation reaction of cyclohexene by **(1A)** in the presence of an excess of triphenylphosphine (PPh_3), 10 times per mol of **(1A)**, does not show any conversion of the hydrogenation product. This result indicates that the real catalyst of the reaction is formed inside the reaction system, and at least a vacant site on the coordination sphere of ruthenium is necessary to promote the hydrogenation of cyclohexene.

To estimate the better reaction time and H_2 pressure, a series of experiments was carried out (see **Fig. 3**). The time dependence of hydrogenation of cyclohexene by complex **(1A)**, in methanol solution, at room temperature and molar ratio cyclohexene/**(1A)** = 500, showed an increase in the hydrogenated product with an increase of time, with 20 atm of H_2. After 5h of reaction, 98% of product (TOF = 98 h^{-1}) was obtained. The catalytic performance of **(1A)** in the methanol solution also increased with the rise of H_2 pressure until 15 atm, keeping constant at 20 atm, also producing 98% of the hydrogenated product, within 5h of reaction.

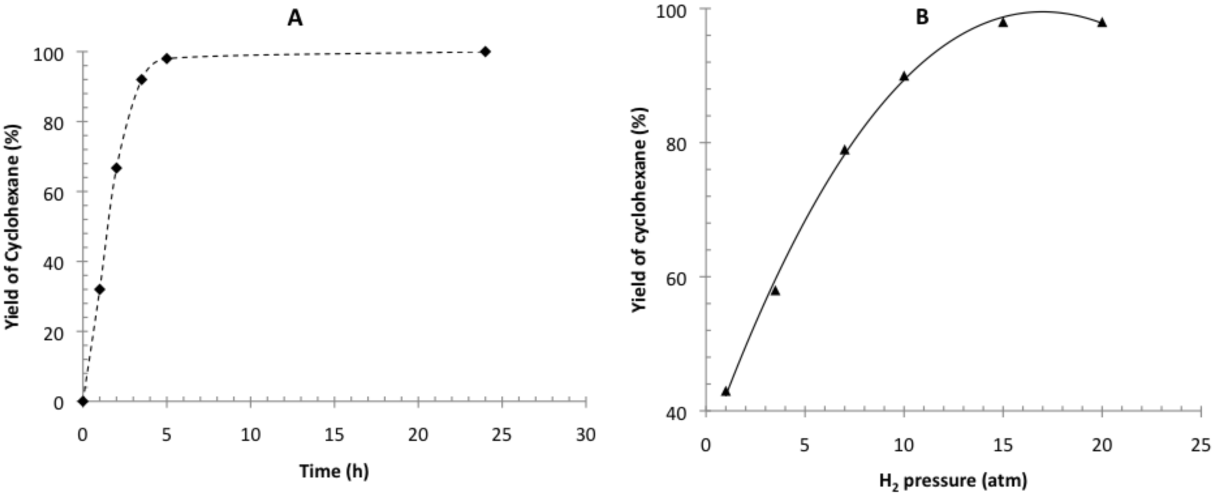

Fig. 3: A) Time dependence of hydrogenation of cyclohexene by **(1A)**. B) Catalytic performance of **(1A)** in the hydrogenation of cyclohexene with an increase of H_2 pressure.

The catalytic productivity of **(1A)** increases with the molar ratio between cyclohexene and **(1A)** until 500. After that, the total amount of the product dropped, but the pre-catalyst **(1A)** still worked at a high conversion rate, with 89 % of product, in the molar ratio at 1/2000, and TOF = 356 h^{-1}. The temperature dependence of hydrogenation of cyclohexene by **(1A)** showed a decrease in the percentage of the hydrogenated product when the temperature was increased. At 25°C, the conversion was quantitative, in the conditions set out above, but the amount of the hydrogenated product decreased to 75% at 80°C. This unusual behavior was attributed to a thermal instability of the complex **(1A)** in this applied condition.

As a protocol for the follow experiments, the hydrogenation reaction of cyclohexene by complexes containing ruthenium **(1A)** – **(11)** was carried out in methanol solution, with 15 atm of H_2 pressure, a molar ratio between cyclohexene/ruthenium complex (S/[Ru]) = 1000, at 25°C, within 5h. Under these conditions, complexes **(1)**, **(2)** and **(3)** provide 100% of the hydrogenated product.

Based on the results obtained from **(1)** – **(3)** on the hydrogenation of cyclohexene, the results obtained with the complexes **(4)** – **(11)** were no surprise, where no catalytic activity was observed. Even after 24 h of reaction, in the best conditions determined by **(1A)**, no catalytic activity was observed. The exchange of chloride for pseudohalide ligands (N_3^-, CN^- and SCN^-) poisoned the catalyst formed inside the system, and due to the strong coordination of these ligands in the ruthenium center, the performance of the pre-catalysts fell drastically. The behavior attributed to the pseudohalide complexes containing ruthenium on the hydrogenation reaction of cyclohexene is practically the same as that described on the hydrogenation reaction with dichloride complexes in the presence of excess of PPh_3. The available catalytic site is lost and the determinant step must pass through an anionic ligand displacement. If this step is prevented from happening, the remained species cannot catalyze the alkene hydrogenation reaction.

4. Conclusion.

The ruthenium complexes *cis*-[Ru(L)$_2$(dppb)(N-N)] {where L = N_3^-, CN^- and SCN^-, N-N = bipy, Me-bipy or MeO-bipy} were prepared by chloride exchange on the *cis*-[RuCl$_2$(dppb)(N-N)] complexes in a mixture of CH_2Cl_2:MeOH (1:1). The pseudohalide complexes were characterized by spectroscopy and electrochemical techniques. Appropriate crystals of *cis*-[Ru(N$_3$)$_2$(dppb)(bipy)], *cis*-[Ru(CN)$_2$(dppb)(bipy)], *cis*-[Ru(SC$\underline{N}$)$_2$(dppb)(bipy)] and *cis*-[Ru(SC$\underline{N}$)$_2$(dppb)(MeO-bipy)] were obtained and the X-ray data were discussed. A total conversion of cyclohexene to cyclohexane was obtain when the *cis*-[RuCl$_2$(dppb)(bipy)], *cis*-[RuCl$_2$(dppb)(Mebipy)] and *cis*-[RuCl$_2$(dppb)(MeObipy)] were used as pre-catalysts. Exchanging chloride for pseudohalides was catastrophic as no catalytic activity was observed. The catalytic poisoning of the compounds with pseudohalides originates from the high stability of these anionic ligands, which prevents the formation of open sites in the coordination sphere of the central atom. Mechanistic studies with compounds 1-3 are underway in our laboratory.

5. Acknowledgment

We would like to thank FAPESP, CNPq, CAPES, FAPEMIG, FINEP, RQ/MG and GMIT for the financial support.

6. Appendix A. Supplementary data.

CCDC 1522479 (**4**), 1522480 (**5**), 1522481 (**6**), 1522482 (**8**) , 1522483 (**11**) and 1523559 (**1B**) contain the supplementary crystallographic data for the complexes *cis*-

$[Ru(N_3)_2(dppb)(bipy)]$**(4)**, *cis*-$[Ru(CN)_2(dppb)(bipy)]$**(5)**, *cis*-$[Ru(SC\underline{N})_2(dppb)(bipy)]$**(6)**, *cis*-$[Ru(CN)_2(dppb)$(Me-bipy)]**(8)** *cis*-$[Ru(SC\underline{N})_2(dppb)$(MeO-bipy)]**(11)** and $[RuCl(CH_3CN)(bipy)(dppb)](PF_6)$ **(1B)** respectively. These data can be obtained free of charge via http://www.ccdc.cam.ac.uk/conts/retrieving.html or from the Cambridge Crystallographic Data Centre, 12 Union Road, Cambridge CB2 1EZ, UK; fax: (+44) 1223 336 033; e-mail: deposit@ccdc.cam.ac.uk. Crystal data (**Table 6S**) and selected bond lengths [Å] and angles [^{o}] for $[RuCl(CH_3CN)(bipy)(dppb)]PF_6$ **(1B)** are described in the supplementary data. Cyclic voltammogram and differential pulse (**Fig.1S**) of *cis*-$[Ru(N_3)_2(dppb)(bipy)]$ **(4)** are depicted in the supplementary data.

7. References

[1] R.A. Sánchez-Delgado, M. Rosales, Kinetic studies as a tool for the elucidation of the mechanisms of metal complex-catalyzed homogeneous hydrogenation reactions, Coord. Chem. Rev. 196 (2000) 249–280. doi:http://dx.doi.org/10.1016/S0010-8545(99)00168-X.

[2] J. Halpern, C.S. Wong, Hydrogenation of tris(triphenylphosphine)chlororhodium(I), J. Chem. Soc., Chem. Commun. (1973) 629–630. doi:10.1039/C39730000629.

[3] A.M. Joshi, K.S. MacFarlane, B.R. James, Kinetics and mechanism of H_2-hydrogenation of styrene catalyzed by $[RuCl(dppb)\ (\mu\text{-}Cl)]_2$ (dppb = 1,4-bis(dipphenylphosphino)butane). Evidence for hydrogen transfer from a dinuclear molecular hydrogen species, J. Organomet. Chem. 488 (1995) 161–

167. doi:http://dx.doi.org/10.1016/0022-328X(94)00016-6.

[4] A.M. Joshi, B.R. James, Characterisation and properties of the dinuclear ruthenium molecular hydrogen complex $[(\eta^2\text{-}H_2)(dppb)Ru(\mu\text{-}Cl)_3RuCl(dppb)]$; dppb = $Ph_2P(CH_2)_4PPh_2$, J. Chem. Soc. Chem. Commun. (1989) 1785–1786. doi:10.1039/C39890001785.

[5] D.E. Fogg, B.R. James, M. Kilner, A comparison of catalytic activity for imine hydrogenation using Ru ditertiary phosphine complexes, including chiral systems, Inorganica Chim. Acta. 222 (1994) 85–90. doi:http://dx.doi.org/10.1016/0020-1693(94)03897-X.

[6] K.S. MacFarlane, I.S. Thorburn, P.W. Cyr, D.E.K.-Y. Chau, S.J. Rettig, B.R. James, Triply-bridged diruthenium(II) 1,4-bis(diphenylphosphino)butane (dppb) and (R)-2,2′-bis(diphenylphosphino)-1,1′-binaphthyl (binap) complexes, including structural characterisation of $[(dppb)\ ClRu(\mu\text{-}D_2O)\text{-}(\mu\text{-}Cl)_2RuCl(dppb)]$, $[(\eta^2\text{-}H_2)\ (dppb)Ru(\mu\text{-}Cl)_3RuCl(dpp$, Inorganica Chim. Acta. 270 (1998) 130–144. doi:https://doi.org/10.1016/S0020-1693(97)05833-7.

[7] M.T. Ashby, J. Halpern, Kinetics and mechanism of catalysis of the asymmetric hydrogenation of alpha,beta-unsaturated carboxylic acids by bis(carboxylato){2,2’-bis(diphenylphosphino)-1,1’-binaphthyl}ruthenium(II), [RuII(BINAP)$(O_2CR)_2$], J. Am. Chem. Soc. 113 (1991) 589–594. doi:10.1021/ja00002a029.

[8] K. Mashima, K. Kusano, T. Ohta, R. Noyori, H. Takaya, Synthesis of new cationic BINAP-ruthenium(II) complexes and their use in asymmetric hydrogenation [BINAP = 2,2'-bis(diphenylphosphino)-1,1'-binaphthyl], J. Chem. Soc. Chem. Commun. (1989) 1208–1210. doi:10.1039/C39890001208.

[9] A.M. Joshi, I.S. Thorburn, S.J. Rettig, B.R. James, Synthesis, characterization and reactivity of some mono- and dinuclear chlororuthenium complexes containing chelating ditertiary phosphines (PP) with PP:Ru=1, Inorganica Chim. Acta. 198–200 (1992) 283–296. doi:https://doi.org/10.1016/S0020-1693(00)92371-5.

[10] J.A. Wiles, C.E. Lee, R. McDonald, S.H. Bergens, [Ru((R)-2,2‘-bis(diphenylphosphino)-1,1‘-binaphthyl)(H)(MeCN)(THF)$_2$](BF$_4$), a Catalyst System for Hydrosilylation of Ketones and for Isomerization, Intramolecular Hydrosilylation, and Hydrogenation of Olefins, Organometallics. 15 (1996) 3782–3784. doi:10.1021/om9603979.

[11] J.P. Genet, S. Mallart, C. Pinel, S. Juge, J.A. Laffitte, General synthesis of novel chiral ruthenium catalysts and their use in asymmetric hydrogenation, Tetrahedron: Asymmetry. 2 (1991) 43–46. doi:http://dx.doi.org/10.1016/S0957-4166(00)82155-2.

[12] D.E. Fogg, B.R. James, Chiral phosphine complexes of ruthenium(II) arenes, J. Organomet. Chem. 462 (1993) C21–C23. doi:http://dx.doi.org/10.1016/0022-328X(93)83387-B.

[13] D.E. Fogg, B.R. James, Chiral and Achiral Diphosphine Complexes of Ruthenium(II) Incorporating Labile Nitrile Ligands: Synthesis and Solution Chemistry of Mono- and Dinuclear Derivatives of $Ru_2Cl_4(PP)_2$ (PP = Chelating Diphosphine), Inorg. Chem. 36 (1997) 1961–1966. doi:10.1021/ic960735y.

[14] J.P. Genêt, C. Pinel, V. Ratovelomanana-Vidal, S. Mallart, X. Pfister, M.C.C. De Andrade, J.A. Laffitte, Novel, general synthesis of the chiral catalysts diphosphine-ruthenium (II) diallyl complexes and a new practical in situ

preparation of chiral ruthenium (II) catalysts, Tetrahedron: Asymmetry. 5 (1994) 665–674. doi:http://dx.doi.org/10.1016/0957-4166(94)80029-4.

[15] I.S. Thorburn, S.J. Rettig, B.R. James, Trichloro-bridged diruthenium(II,III) complexes: preparation, properties, and x-ray structure of $Ru_2Cl_5(chiraphos)_2$ (chiraphos = 2(S),3(S)-bis(diphenylphosphino)butane), Inorg. Chem. 25 (1986) 234–240. doi:10.1021/ic00222a028.

[16] W. Baratta, G. Chelucci, S. Gladiali, K. Siega, M. Toniutti, M. Zanette, E. Zangrando, P. Rigo, Ruthenium(II) Terdentate CNN Complexes: Superlative Catalysts for the Hydrogen-Transfer Reduction of Ketones by Reversible Insertion of a Carbonyl Group into the Ru?H Bond, Angew. Chemie Int. Ed. 44 (2005) 6214–6219. doi:10.1002/anie.200502118.

[17] B.R. James, Synthesis of chiral amines catalyzed homogeneously by metal complexes, Catal. Today. 37 (1997) 209–221. doi:http://dx.doi.org/10.1016/S0920-5861(97)00011-4.

[18] C. Rodrigues, F.G. Delolo, L.M. Ferreira, P.I. Da S Maia, V.M. Deflon, J. Rabeah, A. Brückner, J. Norinder, A. Börner, A.L. Bogado, A.A. Batista, Ruthenium(III)/phosphine/pyridine complexes applied in the hydrogenation reactions of polar and apolar double bonds, J. Mol. Struct. 1111 (2016) 84–89. doi:10.1016/j.molstruc.2016.01.080.

[19] D.A. Cavarzan, F.D. Fagundes, O. Fuganti, C.W.P. Da Silva, C.B. Pinheiro, D.F. Back, A. Barison, A.L. Bogado, M.P. De Araujo, Mixed phosphine/diimines and/or amines ruthenium carbonyl complexes: Synthesis, characterization and transfer-hydrogenation, Polyhedron. 62 (2013) 75–82. doi:10.1016/j.poly.2013.06.022.

[20] T.F. Gallatti, A.L. Bogado, G.V. Poelhsitz, J. Ellena, E.E. Castellano, A.A. Batista, M.P. de Araujo, Heterobimetallic [Ru(II)/Fe(II)] complexes: On the formation of trans- and cis-[$RuCl_2$(dppf)(diimines)], J. Organomet. Chem. 692 (2007) 5447–5452. doi:10.1016/j.jorganchem.2007.08.038.

[21] M.P. De Araujo, A.T. De Figueiredo, A.L. Bogado, G. Von Poelhsitz, J. Ellena, E.E. Castellano, C.L. Donnici, J.V. Comasseto, A.A. Batista, Ruthenium phosphine/diimine complexes: Syntheses, characterization, reactivity with carbon monoxide and catalytic hydrogenation of ketones, Organometallics. 24 (2005) 6159–6168. doi:10.1021/om050182b.

[22] C. Rodrigues, F.G. Delolo, J. Norinder, A. Börner, A.L. Bogado, A.A. Batista, Hydroformylation-hydrogenation and hydroformylation-acetalization reactions catalyzed by ruthenium complexes, J. Mol. Catal. A Chem. 426 (2017) 586–592. doi:10.1016/j.molcata.2016.09.020.

[23] A.L. Bogado, R.F. De Souza, U. Schuchardt, A.A. Batista, On the kinetics of epoxidation of olefins by cis and trans-[$RuCl_2$(dppb)(2,2′-bipy)] complexes, J. Mol. Catal. A Chem. 203 (2003) 129–135. doi:10.1016/S1381-1169(03)00353-4.

[24] L.L. Romualdo, A.L. Bogado, E.M.A. Valle, I.S. Moreira, J. Ellena, E.E. Castellano, M.P. de Araujo, A.A. Batista, Novel manganese (III) porphyrin containing peripheral “[RuCl(dppb)(X-bipy)]$^{+}$” cations [dppb = 1,4-bis(diphenylphosphino)butane and X = -CH_3, -OMe, -Cl]. X-ray structure of the cis-[RuCl(dppb)(bipy)(4-Mepy)]PF_6 complex, Polyhedron. 27 (2008) 53–58. doi:10.1016/j.poly.2007.08.021.

[25] S.L. Queiroz, A.A. Batista, G. Oliva, M.T. do Pi. Gambardella, R.H.A. Santos, K.S. MacFarlane, S.J. Rettig, B.R. James, The reactivity of five-coordinate Ru(II)

(1,4-bis(diphenylphosphino)butane) complexes with the N-donor ligands: ammonia, pyridine, 4-substituted pyridines, 2,2′-bipyridine, bis(o-pyridyl)amine, 1,10-phenanthroline, 4,7-diphenylphenanthroline and ethylened, Inorganica Chim. Acta. 267 (1998) 209–221. doi:https://doi.org/10.1016/S0020-1693(97)05615-6.

[26] M.A.P. Almeida, F.B. do Nascimento, A.E. Graminha, A.G. Ferreira, J. Ellena, F.M. dos S. Mello, A.P. de Lima, E. de P. Silveira-Lacerda, A.A. Batista, Structural features and cytotoxic activities of [Ru(AA-H)(dppb)(bipy)]PF_6 complexes, Polyhedron. 81 (2014) 735–742. doi:https://doi.org/10.1016/j.poly.2014.07.024.

[27] M.I. Frazão Barbosa, E.M.A. Valle, S.L. Queiroz, J. Ellena, E.E. Castellano, V.R.S. Malta, J.R. de Sousa, O. Piro, M.P. de Araujo, A.A. Batista, On the synthesis and structures of the complexes [RuCl(L)(dppb)(N–N)]PF_6 (L = CO, py or 4-NH_2py; dppb = 1,4-bis(diphenylphosphino)butane; N–N = 2,2′-bipyridine or 1,10-phenanthroline) and [(dppb)(CO)Cl2-Ru-pz-RuCl_2(CO)(dppb)] (pz = pyrazine), Polyhedron. 29 (2010) 2297–2303. doi:https://doi.org/10.1016/j.poly.2010.04.028.

[28] K.M. De Oliveira, T.C.C. Dos Santos, L.R. Dinelli, J.Z. Marinho, R.C. Lima, A.L. Bogado, Aggregates of gold nanoparticles with complexes containing ruthenium as modifiers in carbon paste electrodes, Polyhedron. 50 (2013) 410–417. doi:10.1016/j.poly.2012.11.014.

[29] V.F. Ferreira, C.R.A. Do Prado, C.M. Rodrigues, L. Otubo, A.A. Batista, J.W. Da Cruz, J. Ellena, L.R. Dinelli, A.L. Bogado, Modified glassy carbon electrode with AuNPs using cis-[RuCl(dppb)(bipy)(4-vpy)]$^+$ as crossed linking agent,

Polyhedron. 78 (2014) 46–53. doi:10.1016/j.poly.2014.04.024.

[30] L.C.M. Souza, T.A. Santos, C.R.A. Do Prado, B.A. V Lima, R.S. Correa, A.A. Batista, L. Otubo, J. Ellena, L.T. Ueno, L.R. Dinelli, A.L. Bogado, Influence of gold nanoparticles applied to catalytic hydrogenation of acetophenone with cationic complexes containing ruthenium, RSC Adv. 6 (2016) 53130–53139. doi:10.1039/C6RA05616D.

[31] A.L. Bogado, R.M. Carlos, C. Daólio, A.G. Ferreira, M.G. Neumann, F. Rominger, S.P. MacHado, J.P. Da Silva, M.P. De Araujo, A.A. Batista, Observation of vinylidene emission in mixed phosphine/diimine complexes of Ru(II) at room temperature in solution, J. Organomet. Chem. 696 (2012) 4184–4190. doi:10.1016/j.jorganchem.2011.09.017.

[32] Enraf-Nonius, Collect; Nonius: Delft, The Netherlands, n.d.

[33] Z. Otwinowski; W. Minor, Processing of X-ray Diffraction Data Collected in Oscillation Mode, Methods in Enzymology, New York, 1997.

[34] R.H. Blessing, An empirical correction for absorption anisotropy, Acta Crystallogr. Sect. A. 51 (1995) 33–38. doi:10.1107/S0108767394005726.

[35] G.M. Sheldrick, Program for Crystal Structure Resolution, (1997).

[36] G.M. Sheldrick, SHELXL-97, Progam for Crystal Structure Analysis, (1997).

[37] L.J. Farrugia, ORTEP-3 for Windows - a version of ORTEP-III with a Graphical User Interface (GUI), J. Appl. Crystallogr. 30 (1997) 565. doi:10.1107/S0021889897003117.

[38] P. van der Sluis, A.L. Spek, BYPASS: an effective method for the refinement of

crystal structures containing disordered solvent regions, Acta Crystallogr. Sect. A. 46 (1990) 194–201. doi:10.1107/S0108767389011189.

[39] Marvin was used for drawing and displaying chemical structures and reactions, chemAxon, Marvin 17.12.0., (2017). http://www.chemaxon.com.

[40] R.M.C. Brito, A.A. Batista, J. Ellena, E.E. Castellano, I.C.N. Diógenes, L.G. de F. Lopes, J.R. de Sousa, Í. de S. Moreira, Synthesis, characterization and crystal structure of a novel thiocyanate–ruthenium(II) complex, Inorg. Chem. Commun. 10 (2007) 1515–1517. doi:https://doi.org/10.1016/j.inoche.2007.09.024.

[41] J.D. Lee, Concise Inorganic Chemistry, 5th ed., Loughborough, 1999.

[42] R.L.K. J. E. Huheey, E. A. Keiter, Inorganic Chemistry, 4 th, HarperCollins College Publishers, New York, NY, 1993.

[43] C.A. Bignozzi, S. Roffia, C. Chiorboli, J. Davila, M.T. Indelli, F. Scandola, Oligomeric dicyanobis(polypyridine)ruthenium(II) complexes. Synthesis, spectroscopic, and photophysical properties, Inorg. Chem. 28 (1989) 4350–4358. doi:10.1021/ic00323a014.

[44] C.A. Bignozzi, F. Scandola, Cyano-bridged ruthenium(II)/platinum(II) complexes: synthesis, photophysical properties, and excited-state redox behavior, Inorg. Chem. 23 (1984) 1540–1545. doi:10.1021/ic00179a015.

[45] S. Kämper, A. Paretzki, J. Fiedler, S. Záliš, W. Kaim, Solar Cell Sensitizer Models [Ru(bpy-R)$_2$(NCS)$_2$] Probed by Spectroelectrochemistry, Inorg. Chem. 51 (2012) 2097–2104. doi:10.1021/ic201825h.

[46] R.H. Herber, G. Nan, J.A. Potenza, H.J. Schugar, A. Bino, Bis(2,2’-

bipyridine)bis(isothiocyanato)ruthenium. Solvate (solvate = acetonitrile, DMSO) and related compounds: crystal structure, VTFTIR and NMR study, Inorg. Chem. 28 (1989) 938–942. doi:10.1021/ic00304a026.

[47] R. Compton, H.K. Gerardi, D. Weidinger, D.J. Brown, W.J. Dressick, E.J. Heilweil, J.C. Owrutsky, Spectra and relaxation dynamics of the pseudohalide (PS) vibrational bands for Ru(bpy)2(PS)2 complexes, PS=CN, NCS and N_3, Chem. Phys. 422 (2013) 135–142. doi:http://dx.doi.org/10.1016/j.chemphys.2012.11.015.

[48] L. Fodor, G. Lendvay, A. Horváth, Solvent Dependence of Absorption and Emission Spectra of $Ru(bpy)_2(CN)_2$: Experiment and Explanation Based on Electronic Structure Theory, J. Phys. Chem. A. 111 (2007) 12891–12900. doi:10.1021/jp075615y.

[49] P. Belser, A. Vonzelewsky, A. Juris, F. Barigelletti, V. Balzani, Excited-State Properties of Some New Ruthenium (II) Cyano-Polypyridine Complexes in Various Solvents, Gazz. Chim. Ital. 115 (1985) 723–729.

[50] S. Tazuke, H.-B. Kim, N. Kitamura, Excited State Behaviors of Ruthenium(II) Complexes as Studied by Time Resolved and Temperature and Solvent Dependent Emission Spectra, in: H. Yersin, A. Vogler (Eds.), Photochem. Photophysics Coord. Compd., Springer Berlin Heidelberg, Berlin, Heidelberg, 1987: pp. 113–118. doi:10.1007/978-3-642-72666-8_19.

Graphical Abstract

Synthesis, Characterization and Reactivity of Halides/Pseudohalides and their Complexes Containing Ruthenium II in the Hydrogenation of Cyclohexene, Murillo C. Ribeiro, Rodrigo S. Corrêa, Marília I. F. Barbosa, Javier Ellena, André L. Bogado and Alzir A. Batista

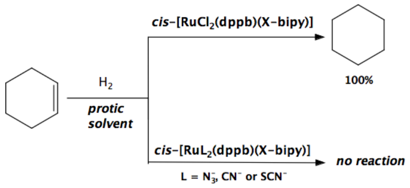

Graphical Abstract - Synopsis

Substituted groups on the 4-position of 2,2′-bipyridine does not influence the total amount of the product on the hydrogenation of cyclohexene. However, exchanging of chloride for pseudohalide (N_3^-, CN^- and SCN^-) detracted the catalyst formed inside the system and no catalytic activity was observed when these complexes were used as pre-catalysts for hydrogenation reactions.